

Thermolubricity of Xe monolayers on graphene

M. Pierno,¹ L. Bignardi,² M.C. Righi,^{3,*} L. Bruschi,¹ S. Gottardi,²
M. Stöhr,² P.L. Silvestrelli,^{1,4} P. Rudolf,^{2,†} and G. Mistura^{1,‡}

¹*Dipartimento di Fisica e Astronomia “G. Galilei” Università di Padova and CNISM
Via Marzolo 8, 35131, Padova, Italy*

²*Zernike Institute for Advanced Materials, University of Groningen
Nijenborgh 4, 9747AG Groningen, The Netherlands*

³*Istituto Nanoscienze, CNR and Dept of Physics, Informatics and Mathematics,
University of Modena e Reggio, 41125 Modena, Italy*

⁴*DEMOCRITOS National Simulation Center, of the Italian Istituto Officina dei Materiali (IOM)
of the Italian National Research Council (CNR), Trieste, Italy*

(Dated: November 18, 2018)

The nanofriction of Xe monolayers deposited on graphene was explored with a quartz crystal microbalance (QCM) at temperatures between 25 and 50 K. Graphene was grown by chemical vapor deposition and transferred to the QCM electrodes with a polymer stamp. At low temperatures, the Xe monolayers are fully pinned to the graphene surface. Above 30 K, the Xe film slides and the depinning onset coverage beyond which the film starts sliding decreases with temperature. Similar measurements repeated on bare gold show an enhanced slippage of the Xe films and a decrease of the depinning temperature below 25 K. Nanofriction measurements of krypton and nitrogen confirm this scenario. This thermolubric behavior is explained in terms of a recent theory of the size dependence of static friction between adsorbed islands and crystalline substrates.

PACS numbers: 68.35.Af, 81.40.Pq, 81.05.ue, 68.65.Pq, 83.10.Rs

Keywords: graphene, nanofriction, thermolubricity, QCM, molecular dynamics, first principles calculations

Since its discovery, graphene has been found to possess numerous outstanding properties such as extreme mechanical strength, extraordinarily high electronic and thermal conductivity, thus opening the way to a plethora of possible applications [1]. In particular, the tribological features of graphene have received increasing attention in view of the development of graphene-based coatings [2]. Graphite is a well-known solid lubricant, used in many practical applications. Its nanofriction behavior has been investigated mainly by frictional force microscopy [3–5]. Measurements on few-layer graphene and single-layer graphene, prepared by micromechanical cleaving on weakly adherent substrates, have revealed that friction monotonically increases as the number of layers decreases [2, 6, 7], while, surprisingly, recent studies showed that this tendency is inverted when graphene is suspended [8].

Here we present the results of a quartz crystal microbalance (QCM) study mainly focused on the sliding of Xe monolayers on graphene (Gr) between 20 and 50 K, a temperature range which has been scarcely investigated in the literature [9], despite its relevance for the formation of condensed two-dimensional phases of many simple gases [10]. In our approach, the gold electrodes of a QCM were covered with Gr because the ample availability of phase diagrams of noble gases monolayers adsorbed on graphite [10] facilitates the interpretation of the QCM sliding measurements [11, 12].

In previous QCM experiments Gr was grown epitaxially on a Ni(111) QCM electrode by heating the QCM to 400 °C in the presence of carbon monoxide [13, 14].

However, no direct morphological characterization of the resulting Gr coating was reported. In our approach, Gr was transferred to the gold QCM electrode with a polymer stamp and fully characterized with a variety of microscopies. Gr was deposited by CVD on an ultra-pure copper foil (purity 99.999%) in a quartz-tube vacuum furnace (base pressure 10^{-5} mbar). The Cu foil was reduced in H₂ (0.5 mbar) and Ar (0.1 mbar) for 60 min at 1180 K. Subsequently Gr was grown by exposing the Cu foil to Ar (0.1 mbar), H₂ (0.5 mbar) and methane (0.5 mbar) for 2 min. at the same temperature [15]. Subsequently, the samples were cooled down to room temperature in an Ar flux. Gr was then transferred onto a polydimethylsiloxane (PDMS) stamp and the copper was etched away with an aqueous solution of FeCl₃. After rinsing with milliQ water and drying in a N₂ flow, the Gr layer was transferred from the PDMS stamp onto the Au electrode of the quartz crystal by applying pressure and peeling the stamp off.

The Gr layer on the Au electrode was characterized by contact-mode atomic force microscopy (AFM). The transferred Gr covered approximately $90 \pm 5\%$ of the electrode surface, as determined by a combination of AFM and optical microscopy. Figure 1-(a) shows a topography AFM micrograph ($3 \times 3 \mu\text{m}^2$) of a Gr-coated area where wrinkles in the Gr layer are clearly visible (blue arrows); the root mean square (RMS) roughness measured on such an area was 3.4 nm. Raman spectroscopy (not shown) indicates that $95 \pm 5\%$ is single layer Gr [16]. Moreover, surface diffraction experiments carried out on layers prepared in the same fashion yield sizes of single-crystalline

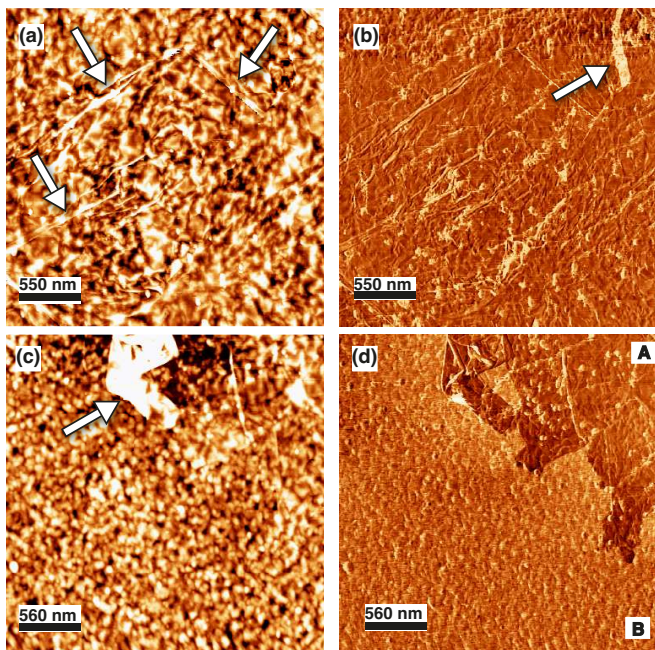


Figure 1: (Color online) Topography (a) and lateral force (b) micrographs of the graphene-coated quartz electrode collected with an atomic force microscope. Brighter regions indicate higher height/friction. In the topography image wrinkles on the surface (blue arrows) are evidence of the presence of graphene. The lateral force micrograph shows homogeneous friction all over the surface, except in correspondence of wrinkles and holes in the graphene (blue arrow). Topography (c) and lateral friction (d) micrographs of an area only partially covered by graphene close to the edge of the gold electrode. The observed features and roughness are comparable to those in panel (a). An area where the graphene is folded is indicated by the arrow. In the lateral friction micrograph (d) region A is covered by graphene while in region B the Au surface is bare.

grains ranging from 100 nm up to 5 μm [16]. Figure 1-(b) presents a lateral force microscopy (LFM) scan of the same area shown in Fig. 1-(a), which appears homogeneous, except along the wrinkles, where the lateral friction is higher. A hole in the Gr membrane (blue arrow) appears as an area with higher friction. Figure 1-(c) shows a topography AFM micrograph of an area at the electrode edge only partially covered by Gr. The roughness of this area is uniform, revealing no differences in topography between covered and uncovered areas, thus suggesting that Gr is adhering to all asperities of the Au electrode. The RMS roughness measured on bare Au is 2.6 nm. Finally, Fig. 1-(d) shows the LFM scan of the same area where two regions with different friction are identified: the low-friction region A corresponds to the Gr coating, the high-friction region B to bare Au, as explained in earlier friction experiments on Gr [6].

Identically prepared Gr-coated quartz crystals were inserted into a QCM mounted and annealed to about 200°C overnight in an UHV chamber housing the cold head of

a 4 K cryocooler [17]. Stainless steel spacers thermally decoupled the QCM holder from the cold head. The adsorbate layer was condensed directly onto the QCM, kept at the chosen low temperature, by slowly leaking high-purity gas through a nozzle facing the quartz electrode. Between consecutive deposition scans, the QCM was warmed up to about 60 K to guarantee full evaporation of Xe and thermal annealing of the microbalance [18]. The slip time τ_s , describing the viscous coupling between substrate and film, can be calculated from the shifts in the resonance frequency and amplitude of the QCM [19]. τ_s represents the time constant of the exponential film velocity decay when the oscillating substrate is brought to a sudden stop. Very low τ_s indicates high interfacial viscosity; if a film is rigidly locked to the substrate, τ_s goes to zero.

Figure 2-(a) shows the slip time of Xe films deposited on Gr at different temperatures, T , and for coverages Θ up to one monolayer (ML). The coverage was deduced from the frequency shift assuming for the ML an areal density of 5.94 atoms/nm², which corresponds to the completion of a solid incommensurate phase on the graphite lattice with nearest-neighbor distance $L_{nn} = 0.441$ nm [10, 13]. This implies a frequency shift for this ML of about 7.6 Hz. For each T , the average of a few runs or the most representative scan is reported for the sake of clarity. Data for $\Theta \leq 0.1$ ML are not plotted because of their intrinsically large fluctuations.

At $T < 30$ K, τ_s is practically zero, indicating that the Xe film is completely pinned to Gr. These findings are consistent with previous studies at low T reporting complete pinning of the highly polarizable N₂, Ar, Kr and Xe and sliding of the weakly polarizable Ne, ⁴He and ³He on different surfaces. [20–25]. At $T = 35$ K, the film is initially pinned to the surface but starts to slide for $\Theta > 0.45$ ML. As the temperature is further increased, τ_s increases monotonically while the depinning onset coverage Θ_{dep} , beyond which the film starts to slide, decreases progressively. At the maximum temperature that could be achieved, $T = 46$ K, the slip time at monolayer completion is ≈ 0.5 ns, much smaller than the value of ≈ 1.7 ns measured at 77 K [13]. This behavior clearly suggests that the sliding of the Xe film is favored by temperature. Similar thermolubric effects have been reported for the friction of a tip moving along a graphite surface [26] and calculated in various models [27].

The slippage of Xe/Gr is significantly different from what observed on bare Au electrodes. As shown in Fig. 2-(b), the Xe slip times measured on Au are much higher than those on Gr and Θ_{dep} is low even at $T = 25$ K. This difference is more evident in Fig. 3, which reports the temperature dependence of Θ_{dep} for all systems. The error bars refer to the standard deviation of data taken in different measurement runs. The vertical dashed line indicates the temperature below which the Xe monolayer is found to be pinned to Gr. These data are indicative

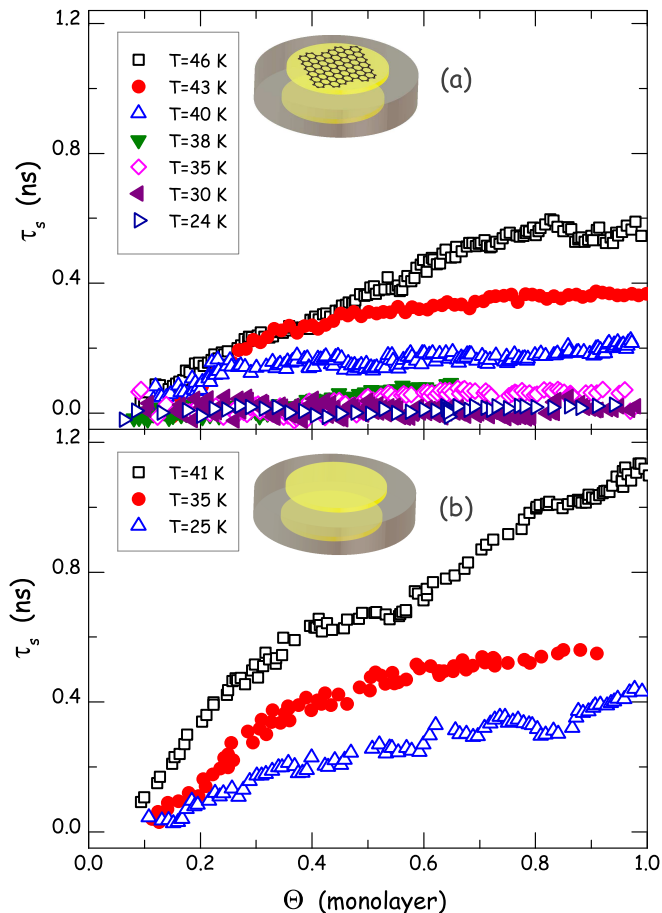


Figure 2: (Color online) Slip time as a function of Xe coverage at different temperatures for (a) Xe on graphene and (b) Xe on gold.

of a thermal depinning transition with a characteristic temperature T_{dep} comprised between 30 and 35 K for Xe/Gr and below 25 K for Xe/Au.

As reported in Fig. 3, a similar trend was also observed for Kr and N_2 films, the only difference being that the characteristic temperatures are shifted to lower values reflecting the smaller polarizability of these adsorbates as compared to Xe. For Kr/Gr, $\Theta_{\text{dep}} \approx 22$ K while, in the case of N_2 , Θ_{dep} cannot be identified due to the narrow temperature range accessible in our experiments. In fact, the data acquisition is limited below, to about 20 K, by the thermal coupling of the QCM to the head of the cryocooler and above, to 24 K, by the evaporation of N_2 at $\Theta_{\text{dep}} \approx 1$. This implies that T_{dep} must be lower than 20 K for both surfaces.

One possible explanation of the observed difference between Gr and Au surfaces is the higher corrugation of the surface potential on Gr with respect to gold. Recent QCM experiments of Xe on a variety of metallic electrodes have verified that the measured slip time is inversely proportional to U_0^2 , where U_0 is the amplitude of the periodic function describing the changes in

adsorbate-substrate potential with respect to adsorbate position [13]. For Xe/Gr, U_0 amounts to 5.3 meV [13] while there is no U_0 value reported in the literature for Xe/Au. We have estimated the corrugation amplitude U_0 for Xe and N_2 on Au and Gr using an *ab-initio* scheme based on the recently-developed nonlocal rVV10 density functionals [28] (including an accurate description of van der Waals effects implemented in the QE package [29]). The interaction of a Xe atom or a N_2 molecule with both the ideal, planar single layer of Gr and the Au(111) surface were considered. The computed U_0 value for Xe/Gr, 2.2 meV, is significantly larger than that for Xe/Au (1.6 meV), thus supporting the explanation of the τ_s data based on the higher corrugation of the surface potential on Gr than on Au. It is worthwhile to point out that, although the absolute values of the *ab-initio* estimates of the corrugation could significantly depend on technical details, such as the chosen density functional, their ratios are expected to be much less sensitive to such particulars and therefore much more reliable. Moreover the experimental estimate of U_0 obtained for Xe/Gr refers to Gr grown on Ni(111) [13], which could explain the discrepancy with our value computed for an ideal, isolated layer of Gr. For N_2 the scenario is similar, since we find U_0 values of 8.0 and 6.6 meV for N_2 /Gr and N_2 /Au, respectively.

As for the observed temperature dependence of τ_s , this is partly consistent with dynamic simulations of the sliding of model Xe layers on weakly corrugated surfaces [27, 30]. The major difference between our data and the aforementioned molecular simulations [30] is the occurrence of a depinning onset coverage which depends on temperature as clearly displayed in Fig. 3 and which contrasts with the sliding at low Θ observed in the simulations. A possible explanation for the observed decrease of Θ_{dep} with temperature relies on a recent theory [31] about the size dependence of static friction between adsorbed islands and crystalline substrates according to which the atomic structure of islands deposited on a substrate of nonmatching lattice parameters consists of commensurate domains separated by incommensurate domain walls. Domain structures are governed by the competition in minimizing both interfacial energy and elastic strain energy. When the size of the contact is reduced below a critical radius, R_c , domains coalesce. This structural transition is accompanied by a sharp increase of the interfacial commensurability and static friction [31]. The depinning of a commensurate interface has been shown to be a thermally activated process with an associated barrier $E_{\text{dep}} \propto \epsilon U_0 (F_s - F) / F_s F$, where F is the applied lateral force and F_s the static friction force [32]. In the case of perfect commensurability, the huge difference between the static friction force and the weak inertia force provided by the oscillating QCM results in a very high activation barrier (for example, $E_{\text{dep}} \simeq 10^7$ eV has been estimated for a Xe monolayer

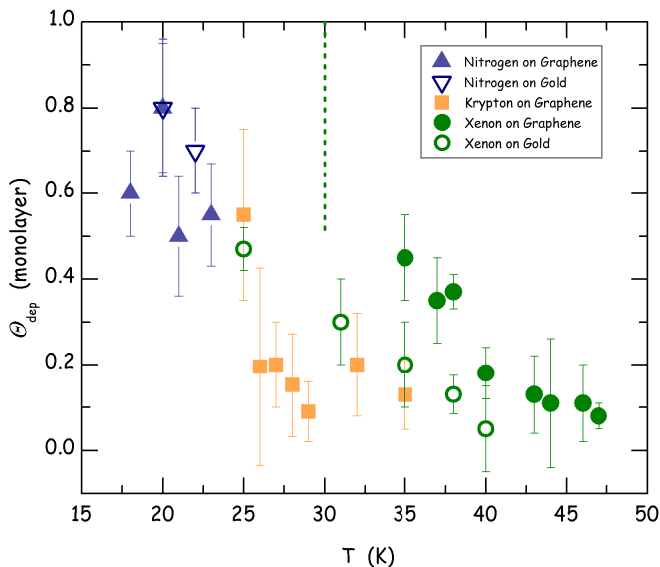


Figure 3: (Color online) Depinning onset coverage as a function of temperature for the systems investigated in this work. Dashed line indicates the temperature below which Xe monolayers are always pinned to graphene. Error bars account for data distributions over different runs performed at different thermal cool downs from room temperature and different surfaces.

on the Cu(111) surface in the absence of defects). Such barrier has been found to drop dramatically by decreasing the interfacial commensurability [32]. By combining these results with the experimental findings, the following interpretation of the QCM data is proposed:

i) The observation of a *thermal activation of the frictional slip* in nominally incommensurate Xe/Gr and Xe/Au systems can be accounted for by the predicted increase of commensurability at small sizes. Islands of radius lower than R_c are expected to be pinned to the QCM, their thermal depinning becoming probable at larger size due to the decrease of static friction, F_s .

ii) The *critical coverage* necessary for the depinning of the film, Θ_{dep} , is related to the coverage necessary for the growing Xe islands to reach a large enough size, $R_{\text{dep}} \geq R_c$, for the depinning process to be activated at the considered temperature. This seems confirmed by the fact that the critical size estimated for Xe on Gr is larger than that on Au in agreement with the experimental observation that Θ_{dep} is larger for Xe/Gr than for Xe/Au (see Fig. 3). The major contribution to the calculated difference in the critical size comes from the different misfit strain e . R_c is, in fact proportional to $1/e^2$ [31], where $e = -0.083$ for Xe/Gr and $e = 0.13$ for Xe/Au [33].

iii) The *temperature dependence of the critical coverage* can be accounted for by the two following arguments. By increasing the temperature, Θ_{dep} decreases because the probability to overcome the barrier E_{dep} increases,

therefore the slip onset is activated for higher values of F_s , that is for smaller island sizes. Furthermore, R_{dep} is reached at lower coverage due to enhanced diffusivity at increased temperature.

This scenario applies not only to Xe/Gr but to all the systems investigated in this work and should be quite general. Realistic temperature dependent simulations of adsorbed films are clearly needed to better clarify the phenomenon of thermal depinning observed in the experiments.

In summary, we have successfully managed to transfer graphene to the gold electrode of a QCM and the adhesion is found to be good even at cryogenic temperatures (e.g. down to 10 K). The presence of graphene on the gold electrode significantly affects the sliding of Xe films. The measured slip time is about half that on bare gold, probably because of the higher corrugation of the surface potential on graphene with respect to gold. Overall, the solid films are found to be rigidly pinned to the surface at sufficiently low temperatures and start sliding at higher temperatures. The onset coverage for sliding decreases with temperature and at a given temperature is smaller on bare gold. Nanofriction measurements on krypton and nitrogen confirm this scenario. This thermolubric behavior is explained in terms of a recent theory of the size dependence of static friction between adsorbed islands and crystalline substrates. This study provides the first direct evidence of thermal lubricity of adsorbed films.

We thank Giorgio Delfitto and Luc Venema for invaluable technical assistance, and Nanolab for the use of the clean-room. This work has been partially supported by the Foundation for Fundamental Research on Matter (FOM) in the framework of the “Graphene-based electronics” research program.

* Electronic address: mcricchi@unimore.it

† Electronic address: p.rudolf@rug.nl

‡ Electronic address: giampaolo.mistura@unipd.it

- [1] K. S. Novoselov, V. I. Falko, L. Colombo, P. R. Gellert, M. G. Schwab, and K. Kim, *Nature* **490**, 192 (2012).
- [2] C. Lee, Q. Li, W. Kalb, X.-Z. Liu, H. Berger, R. W. Carpick, and J. Hone, *Science* **328**, 76 (2010), PMID: 20360104.
- [3] E. Gnecco and E. Meyer, *Fundamentals of Friction and Wear* (Springer, 2007).
- [4] M. Dienwiebel, G. S. Verhoeven, N. Pradeep, J. W. M. Frenken, J. A. Heimberg, and H. W. Zandbergen, *Phys. Rev. Lett.* **92**, 126101 (2004).
- [5] S. Koch, D. Stradi, E. Gnecco, S. Barja, S. Kawai, C. Díaz, M. Alcamí, F. Martín, A. L. Vázquez de Parga, R. Miranda, T. Glatzel, and E. Meyer, *ACS Nano* **7**, 2927 (2013).
- [6] T. Filleter, J. L. McChesney, A. Bostwick, E. Rotenberg, K. V. Emtsev, T. Seyller, K. Horn, and R. Bennewitz, *Phys. Rev. Lett.* **102**, 086102 (2009).

- [7] T. Filleter and R. Bennewitz, Phys. Rev. B **81**, 155412 (2010).
- [8] Z. Deng, N. N. Klimov, S. D. Solares, T. Li, H. Xu, and R. J. Cannara, Langmuir **29**, 235 (2013).
- [9] M. F. Danisman and B. Özkan, Rev. Sci. Instrum. **82**, 115104 (2011).
- [10] L. W. Bruch, R. D. Diehl, and J. A. Venables, Rev. Mod. Phys. **79**, 1381 (2007).
- [11] N. Hosomi, A. Tanabe, M. Suzuki, and M. Hieda, Phys. Rev. B **75**, 064513 (2007).
- [12] N. Hosomi, J. Taniguchi, M. Suzuki, and T. Minoguchi, Phys. Rev. B **79**, 172503 (2009).
- [13] T. Coffey and J. Krim, Phys. Rev. Lett. **95**, 076101 (2005).
- [14] M. Walker, C. Jaye, J. Krim, and M. W. Cole, J. Phys.: Condens. Matter **24**, 424201 (2012).
- [15] C. Mattevi, H. Kim, and M. Chhowalla, J. Mater. Chem. **21**, 3324 (2011).
- [16] L. Bignardi, W. F. van Dorp, S. Gottardi, O. Ivashenko, P. Dudin, A. Barinov, J. T. M. De Hosson, M. Stohr, and P. Rudolf, Nanoscale **5**, 9057 (2013).
- [17] L. Bruschi, A. Carlin, F. Buatier de Mongeot, F. dalla Longa, L. Stringher, and G. Mistura, Rev. Sci. Instrum. **76**, 023904 (2005).
- [18] M. Pierno, L. Bruschi, G. Mistura, C. Boragno, F. B. de Mongeot, U. Valbusa, and C. Martella, Phys. Rev. B **84**, 035448 (2011).
- [19] L. Bruschi and G. Mistura, Phys. Rev. B **63**, 235411 (2001).
- [20] R. L. Renner, P. Taborék, and J. E. Rutledge, Phys. Rev. B **63**, 233405 (2001).
- [21] G. Fois, L. Bruschi, L. d'Apolito, G. Mistura, B. Torre, F. B. de Mongeot, C. Boragno, R. Buzio, and U. Valbusa, J. Phys.: Condens. Matter **19**, 305013 (2007).
- [22] M. Highland and J. Krim, Phys. Rev. Lett. **96**, 226107 (2006).
- [23] L. Bruschi, G. Fois, A. Pontarollo, G. Mistura, B. Torre, F. Buatier de Mongeot, C. Boragno, R. Buzio, and U. Valbusa, Phys. Rev. Lett. **96**, 216101 (2006).
- [24] M. Pierno, L. Bruschi, G. Fois, G. Mistura, C. Boragno, F. B. de Mongeot, and U. Valbusa, Phys. Rev. Lett. **105**, 016102 (2010).
- [25] T. Oda and M. Hieda, Phys. Rev. Lett. **111**, 106101 (2013).
- [26] K. B. Jinesh, S. Y. Krylov, H. Valk, M. Dienwiebel, and J. W. M. Frenken, Phys. Rev. B **78**, 155440 (2008).
- [27] A. Vanossi, N. Manini, M. Urbakh, S. Zapperi, and E. Tosatti, Rev. Mod. Phys. **85**, 529 (2013).
- [28] R. Sabatini, T. Gorni, and S. de Gironcoli, Phys. Rev. B **87**, 041108(R) (2013).
- [29] <http://www.quantum-espresso.org>.
- [30] B. N. J. Persson, Phys. Rev. B **48**, 18140 (1993).
- [31] M. Reguzzoni and M. C. Righi, Phys. Rev. B **85**, 201412 (2012).
- [32] M. Reguzzoni, M. Ferrario, S. Zapperi, and M. C. Righi, Proc. Nat. Acad. Sci. **107**, 1311 (2010).
- [33] The misfit strain is calculated as $e = (a' - b)/b$, where b is the lattice parameter of an unstrained Xe layer and a' is the parameter of the substrate sub-lattice occupied by the Xe atoms in a commensurate configuration. We considered a $\sqrt{3} \times \sqrt{3}$ sub-lattice, therefore $a' = \sqrt{3}a$, with a parameter of the hexagonal substrate surface.